

# We are IntechOpen, the world's leading publisher of Open Access books Built by scientists, for scientists

6,900

Open access books available

185,000

International authors and editors

200M

Downloads

Our authors are among the

154

Countries delivered to

TOP 1%

most cited scientists

12.2%

Contributors from top 500 universities



WEB OF SCIENCE™

Selection of our books indexed in the Book Citation Index  
in Web of Science™ Core Collection (BKCI)

Interested in publishing with us?  
Contact [book.department@intechopen.com](mailto:book.department@intechopen.com)

Numbers displayed above are based on latest data collected.  
For more information visit [www.intechopen.com](http://www.intechopen.com)



---

# Diabetes Ground Control: A Novel System for Correcting Anomalous Stride in Diabetic Patients

---

Suélia de Siqueira Rodrigues Fleury Rosa,  
Mário Fabrício Fleury Rosa,  
Marcella Lemos Brettas Carneiro, Leticia Coelho,  
Diego Colón and Célia Aparecida Reis

Additional information is available at the end of the chapter

<http://dx.doi.org/10.5772/intechopen.74040>

---

## Abstract

Diabetes mellitus is a chronic disease characterized by several complications, including diabetic foot, a serious problem induced by increased foot plantar pressure during gaiting. This misbehavior intensifies the risk of ulceration, which may lead to minor and major amputations. This study proposes the inclusion of a passive element to correct diabetic stride, namely the Diabetes Ground Control (DGC), a customized latex-based insole designed to perform load redistribution along the entire foot length, and by so minimizing overload and pressure levels on the foot sole of diabetic patients. A mathematical model in state space for the DGC system is proposed and dynamically characterized using polynomial chaos analysis. The inclusion of the DGC element reduced considerably the amplitude of foot pressure oscillations during walking. Hence, the DGC, which can be customized according to the patient's physical characteristics and weight, is a potential instrument for controlling the tensions on the diabetic foot.

**Keywords:** diabetic foot, bond graph, polynomial chaos, biomechanics, organic control, latex

---

## 1. Introduction

Diabetic foot is a pathophysiological state associated with the appearance of ulcers, infections, and/or destruction of deep tissues, observable in patients with diabetes mellitus (DM). These symptoms occur as a consequence of neuropathy, peripheral vascular disease, or deformities in lower limbs [1–4].

The diabetic foot is a very debilitating complication of the DM, which often leads to ulcerations that can evolve to minor or major amputations [5]. The injuries can appear in different places such as in the toes, due to high external pressures caused by muscle atrophy, in interdigital skin, as a result of fissures and small cuts that favor the colonization by skin fungus, in distal parts of the foot, where the prominences of the metatarsus, when ulcerated, can originate infection outbreaks that can penetrate phalangeal articulations and thus leading to infections, and in the middle portion of the foot, where callosities and injuries can be developed since this is the area responsible for body support [2, 6–9]. According to El-Hilaly et al. [5], each patient should receive personalized treatment, since there are always individual differences in pressure values, pressure distribution, foot deformities, and soft tissue thickness and integrity. Usually, there is a decrease in the accuracy of gait movement due to variations on pelvic angles, reduced speed of muscle activation, reduced gait speed, reduced movement capability, smaller step amplitude, and greater impact absorption by the foot [4, 10–12].

The vast majority of design strategies and selection criteria for suitable insoles for diabetics rely mainly on experience and intuition of the shoemakers rather than on design techniques based on scientific principles. A shoe design must protect the foot in locations that are at risk of developing lesions, by reducing pressure to values below specific thresholds, to avoid ulcerations. Some authors have used insoles with pressure sensors for indicating and correcting plantar pressure distribution, through adjustments in footwear and commercial insoles. These insoles have hexagonal-shaped plugs, with the possibility of removing pieces to promote plantar pressure relief in a region such as the metatarsal point [13, 14]. This system, known to be the most personalized gadget available in the market for the correction of the diabetic gait, still does not consider all the evidences of muscular deficit and corresponding cinematic decreases in the prevention and treatment of diabetic foot.

The main reason for the absence of general design criteria for therapeutic shoes is the wide range of patient characteristics and the high number of design variables. Therefore, presenting a mathematical model for the diabetic gait is essential for understanding the mechanical parameters, for the analysis of pressure data, and for gaiting control through the usage of customized insoles. Specifically, we believe that characterizing the influence of a damper on the distribution and dynamics of the foot sole allows a clearer understanding of the diabetic stride, by clarifying its interference in the distribution of pressure and its role in reducing impacts during the process of walking.

Based on the mechanical etiology of the problem, this chapter proposes the inclusion of an external element, namely the Diabetes Ground Control (DGC) insole, to change the forces of contact between ground and foot, aiming to minimize overload and pressure levels in the patients' foot sole. This controlled interaction between the diabetic foot and the device is what the authors claim as the concept of Organic Control. Specifically, the passive controller actively modifies the system response through the redistribution of the load along the entire length of the foot. The sensibility/robustness of the system is then analyzed by the method of polynomial chaos. It will be used to evaluate the poles dispersion by the introduction of the DGC.

## 2. Material and methods

### 2.1. Data collection and analysis procedures

One female individual (age: 33 years, height: \*\*\* cm, mass: \*\* kg) volunteered for this investigation and gave her informed written consent. The volunteer has Diabetes Type 1 (diagnosed 24 years ago), has communication and locomotion capabilities, and uses insulin pumps. The research protocol was approved by the Research Ethics Committee from the Federal District's Health Department (SES/DF) under the following protocol number: 428/11.

Before the data collection, the volunteer answered a structured questionnaire with close-ended questions (birth date, gender, date of diagnosis, type of medication, type of DM, and others) and the questionnaire provided by the Michigan Neuropathy Screening Instrument (instrument that evaluates the symptoms related to the diabetic neuropathy). After that, we carried out an interview to collect data regarding the characterization of the patient's gait conditions, taking into consideration a possible difficulty to walk. We measured her height, weight, basal temporal dose, heartbeat, oxygen saturation, anthropomorphic dimensions of the foot (with a caliper), and glycemic index—with the Accu-Chek® Active lancing device (Hoffmann-La Roche, Basel Switzerland). Then, the patient was asked to answer a questionnaire destined to assess her quality of life and her motor skills (e.g. walking, climbing stairs, driving a car, performing household chores), as well as aspects related to financial considerations, medication side effects, and lifestyle (general dimensions). The participant was advised not to consume alcohol or any kind of medication 24 h prior to the commencement of the experiment. The participant was also advised about the experiment and given a trial run before the readings were taken.

Since the method includes the use of a custom-made insole with sensors, some measurements were performed to collect data that would allow the optimization of the insole. To determine where the sensors would be placed, we performed a pedographic analysis using the Emed® n50 Novel platform (Novel, Munich, Germany), which allows for the collection of plantar pressure distribution data, which consists of sensors and circuits for data collection as well as control software. The patient, barefoot and with her eyes open, was asked to remain for 30 s in an orthostatic position and to distribute her body weight evenly between both feet. Afterwards, we attached, to one of the patient's feet, a system designed to capture and record the signal generated by four strength sensors. The system was controlled by the EZ430-F2013 development kit by Texas Instruments, which is equipped with the MSP430 controller and with a Wi-Fi module for data transmission. The system's sampling rate is 40 Hz. The circuit that conditions the pressure outputs are connected to the A/D converter embedded in the microcontroller, which sends the data to the computer via Wi-Fi. Software was developed to control the data acquisition from the insole, to send and receive messages containing these data, to allow for the reading of the elements by MatLab and, finally, to present the information obtained. Four FlexiForce® sensors by Tekscan, model HT 201 (Tekscan, South Boston, USA), were used. The sensors were attached to the insole with a tape so that they could not move during the tests. With the insole attached to the patient's foot, we began the collection of

the data. In the experimental procedure, the volunteer stood still for 10 s, walked for about 50 s, and then stopped again for 30 s. Another similar collection was carried out to generate validation data. The insole, made of natural latex (biomaterial), is, differently from other insoles with plantar pressure measurement systems, fabricated to be completely individualized and customized, following the anatomy and the characteristics of the patient's feet. Because of this, in order to capture the plantar pressure values, the sensors were placed in specific parts of the foot. **Figure 1a** shows the plantar distribution of the sensors and **Figure 1b** shows the acquisition system, consisting of FlexiForce® sensors connected to a data acquisition board with a buffer, and a gain stage connected to the microcontroller Msp430f2274 (rf2500), and the natural latex insole. We highlight that the alterations in the trajectory of the center of pressure (COP) in the medial-lateral direction, in neuropathic individuals, as shown in **Figure 1a**, is an important factor when using a customized insole.

## 2.2. Manufacturing of the insole

Most diabetic insoles available on the market are composed of silicon, polyurethane, ethylene-vinyl acetate (EVA), or memory foam. We, nevertheless, chose to work with latex. This biomaterial, which is a milky sap and a living organism before vulcanization, is obtained from a tree called *Hevea brasiliensis*, represents a durable, low-cost and high-quality raw material with physical and chemical characteristics that are biocompatible. It is also known for its antigenicity, hypoallergenicity, impermeability, elasticity, softness, flexibility, and resistance. Latex has been utilized in the past for the manufacturing of esophageal prosthesis, bio-membranes and modules for the control of esophageal flow, as described by Rosa and Altoé [15] and Andrade [16].

The abovementioned characteristics, which diabetic insole materials must present, are in accordance with the latest scientific studies and aim to provide patients with a more comfortable

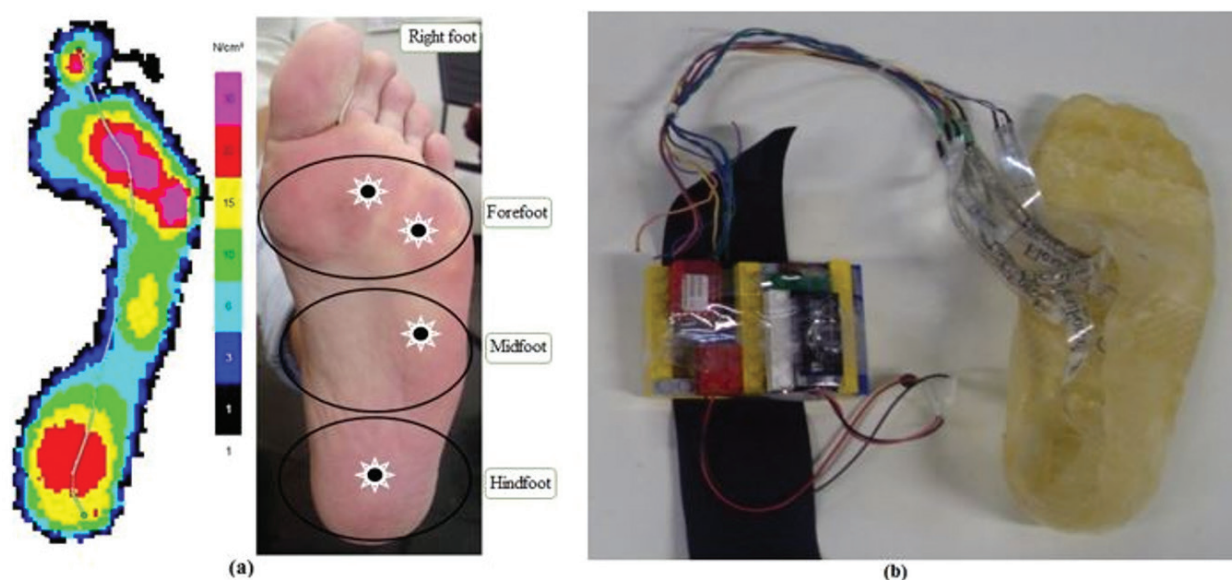


**Figure 1.** Distribution of the sensors for the capture of data in the identification of the model. (a) Image from the pedographic essay that shows the plantar pressure ( $\text{N}/\text{cm}^2$ ), the color map and the center of pressure trajectory composed by innumerable displacements in the sagittal plane; (b) disposition of the sensors on the patient's foot.

experience, including concerns with the feet temperature control and the reduction of allergy risks. Therefore, latex will be the constituent of the dampers on the insole with its mechanical properties changed according to the foot temperature. This interaction between the foot and the latex insole occurs as a symbiotic relationship and will be the foundation of the bioinspired system under study.

In the manufacturing process of the insole, the technique of successive immersion baths was applied, in which the mold is slowly plunged, on a perpendicular position, into the final latex compound, and then heated in a thermostatically controlled kiln. The first step consists of washing the mold with water and soap. Then, the mold has to be dried with hot air, sterilized in an autoclave (heated in the kiln at a temperature of 50°C), removed, and, then, plunged into the latex, where it should remain for 1 min. This step represents the beginning of the polymerization that determines the final manufacturing of the product. After this phase, the molds will be slowly and gradually removed from the latex compound and put into the kiln (subject to heating for vulcanization at a temperature of 70°C) for 10 min. After this, the mold is kept for 20 more min out of the kiln. We highlight that the bathing and heating steps will be repeated until we can obtain a thickness of approximately 3 mm for the insole. By the end of the process, we place the insole under running water to remove it from its mold. According to the literature, by diluting latex—at a temperature of 25°C—in double-distilled water we obtain at 30% an  $\eta$  (25°C) = 15 centipoise or 0.02 N s/m<sup>2</sup>. The  $\tau$  on the front portion of the foot corresponds to the ratio between the weight force and the rectangle's area (0.05 m × 0.032 cm), that is,  $\tau = 42.875103$  N/m<sup>2</sup>. The shear rate is given by 21.43106 m<sup>2</sup>/s of how much the latex layers in the shock absorber 'slide' over each other. It was based on this value that we determined the percentage of water required to alter the viscosity of the latex. Because viscosity is considered non-constant and must be altered for each patient, we could not obtain a flow curve.

### 2.3. Modeling by bond graph

The *Bond Graph* (BG), which is an alternative method to the classical existing modeling practices, has been used for obtaining a mathematical model for the presented system. As usual in BG modeling, some assumptions were made in the mathematical modeling, in order to avoid high and unnecessary complexity. These are (1) The developed models are only approximate representations, and there is no single model of the system, but rather a family of models with varying features and performances; (2) The static (damping) force of Coulomb friction is considered to be negligible; (3) The effect of the Lagrange equation ( $\delta q_i$ ) is considered to be a non-infinitesimal virtual displacement; (4) The displacement of elements (deflection) is referred to by  $\delta$  in steady state; (5) The surface where the subject walks is fixed, that is, it will be considered to have no misalignments (holes and steps) and an angle will be assigned for situations with ascending or descending movement; (6) There will be no rotation around the axes, only the translational movement will be worked on; (7) The system is considered to be symmetric, and only the right leg is modeled; (8) The model is of the concentrated parameters type.

The BG models proposed for the system were constructed using the 20-sim simulation software. The purpose of the system is to represent the reductions in kinematic variables, such as displacement, velocity, acceleration, and linear momentum. Mass (M1), the frontal part of

foot, is connected in series with a spring (K1) and a damper (B1), parameter of the foot/leg, representing the greater impact that body weight has in the frontal part of foot during passive diabetic stride. For representing the lag in the activation of the muscles that directly influence the COP, we use a damper (B1), accounting for the angle (ankle-joint) reduction and a low torque. Finally, at the heel region, responsible for propelling the movement, a spring (K2) was used to demonstrate the deformation of the movement. In both cases, in the compression of the spring and in its movement back to its equilibrium length, the force is always in the opposite direction of the movement, and was proportional to the displacement in this study.

One of the symptoms of the diabetes mellitus is the gradual change in the patient’s normal stride. These deviations or distortions ( $\pm \delta$ ) can appear in several mechanical elements of the model. We incorporated these distortions into masses (M0 and M1), springs (K1 and K2) and damper (B1). The distortion is like an imperfect coupling of impedance (impedance mismatch) that generates a loss of signal strength (or amplitude) at the angle of the ankle joint, stride height, and muscle strength (B1 and M1). It is also responsible for the shock on the frontal part of the foot (M1) and the low amplitude of its velocity. Therefore, these variables change their reference from point to surface, which implies the deflection that generates the delay displayed on the mathematical formulation of the system.

Diabetic person’s foot in descent/ascent movement can be modeled by changing its spatial position, here represented by an inclined plane. The influence of the force decomposed into rectangular coordinates generates a dependency that is directly proportional to inclined plane angle  $\beta$ . Furthermore, delays in the stride are recurring, and the person needs to make small stops and then resume walking. In this analysis, we also incorporated in the control system a saturating element (hysteresis) to account for this behavior. **Figure 2** presents the system with its ideal physical model and the complete BG model without simplification.

The corresponding state space representation is given by the following equations:

$$\begin{pmatrix} \dot{x}_1 \\ \dot{x}_2 \\ \dot{x}_3 \\ \dot{x}_4 \end{pmatrix} = \begin{pmatrix} -\frac{A}{M_0} & -K_2 \cos^2 \beta & -K_1 \cos^2 \beta & \frac{A}{M_1} \\ \beta & 0 & 0 & 0 \\ \beta & 0 & 0 & -\beta \\ \frac{A}{M_0} & 0 & K_1 \cos^2 \beta & -\frac{A}{M_1} \end{pmatrix} \begin{pmatrix} x_1 \\ x_2 \\ x_3 \\ x_4 \end{pmatrix} + \begin{pmatrix} 1 \\ 0 \\ 0 \\ 0 \end{pmatrix} \quad (1)$$

$$y = (0 \ 0 \ 0 \ 1) \begin{pmatrix} x_1 \\ x_2 \\ x_3 \\ x_4 \end{pmatrix} \quad (2)$$

$$A = \frac{(1 - e^{-\alpha v})^{-1} (b v + 1) * \text{sen} \beta}{\frac{1}{12} r^2 \text{g sen} \beta} \quad (3)$$

$$B = \frac{1}{\frac{1}{12} M_0 . r^2 \text{g sen} \beta} \quad (4)$$

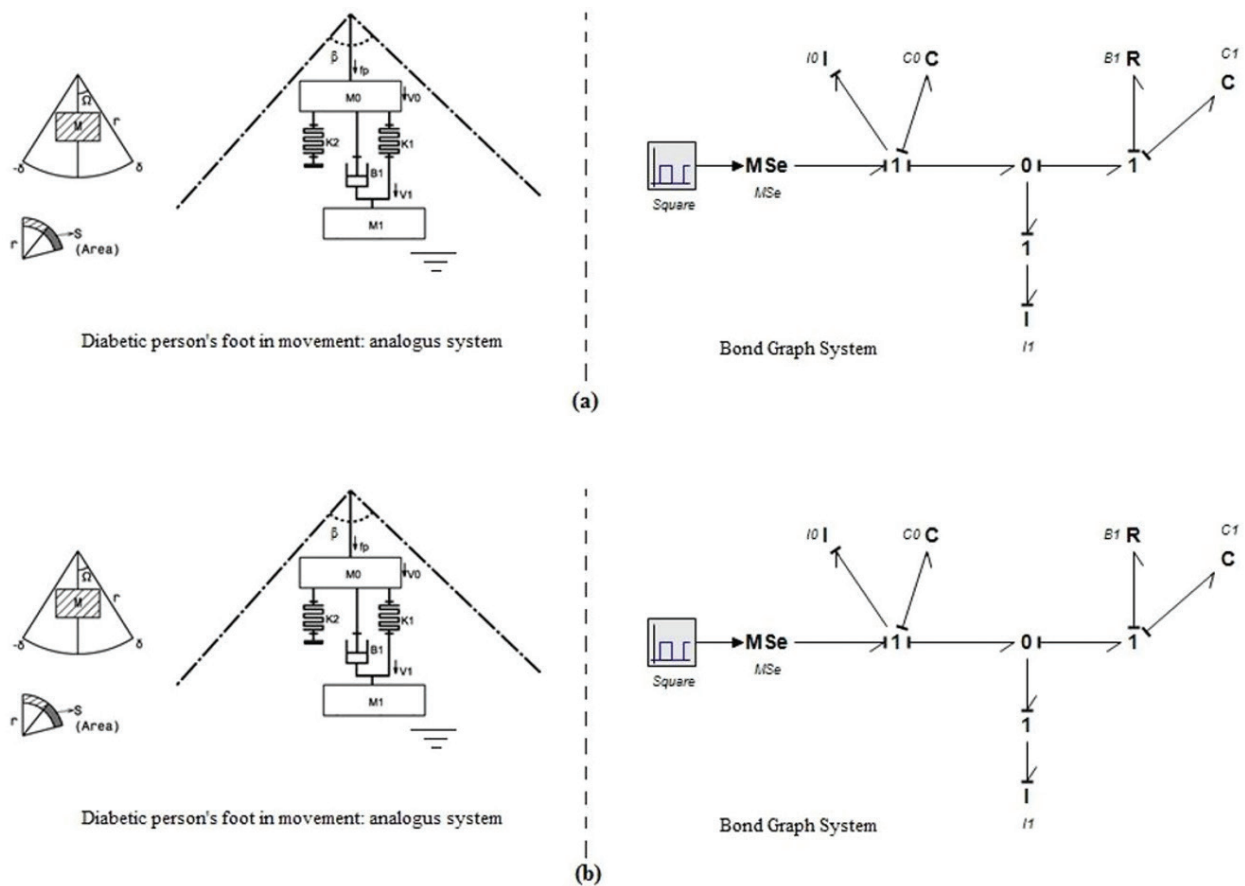


**Figure 2.** The right foot in the passive diabetic stride. The frontal part of the foot is the dashed line. It is considered that, in (a), the situation is the foot of a person with diabetes in descendent/ascendant movement with deflection ( $\pm \delta$ ), highlighting the visualization area and (b) complete BG model.

where  $x_1(t)$   $x_1(t)$  represents the velocity of mass  $M_0$ ,  $x_2(t)$  corresponds to the displacement of spring  $K_1$ ,  $x_3(t)$  to the displacement of spring  $K_2$ , and  $x_4(t)$  the velocity of mass  $M_1$ .

We then derived a second model that includes the customized insole made of latex, the DGC element. It was modeled using two additional shock absorbers  $B_2$  and  $B_3$  in series with  $M_1$  and the corresponding mass of the customized insole ( $M_2$ ). **Figure 3** shows the mechanical analog and complete BG model for the DGC system.

The resulting state space representation for the DGC system is given by Eqs. (5) and (6):

$$\begin{pmatrix} \dot{x}_1 \\ \dot{x}_2 \\ \dot{x}_3 \\ \dot{x}_4 \\ \dot{x}_5 \end{pmatrix} = \begin{pmatrix} -\frac{B_1}{M_0} & -K_1 & -K_2 & \frac{B_2}{M_1} & 0 \\ \frac{1}{M_0} & 0 & 0 & -\frac{1}{M_1} & 0 \\ \frac{1}{M_0} & 0 & 0 & -\frac{1}{M_1} & 0 \\ \frac{B_1}{M_0} & K_1 & K_2 & -\frac{B_2}{M_1} - \frac{B_2 B_3}{(B_2 + B_3) M_2} & \frac{B_2 B_3}{(B_2 + B_3) M_2} \\ 0 & 0 & 0 & \frac{B_2 B_3}{(B_2 + B_3) M_1} & -\frac{B_2 B_3}{(B_2 + B_3) M_2} \end{pmatrix} \begin{pmatrix} x_1 \\ x_2 \\ x_3 \\ x_4 \\ x_5 \end{pmatrix} + \begin{pmatrix} 1 \\ 0 \\ 0 \\ 0 \\ 0 \end{pmatrix} M_{se} \quad (5)$$

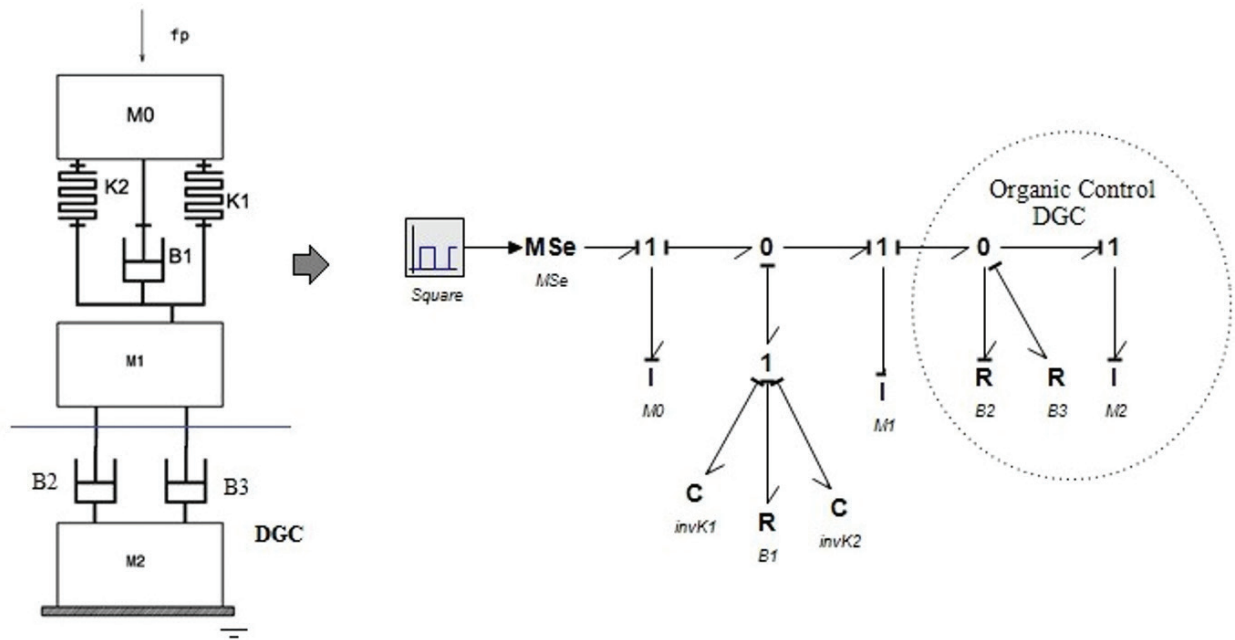


Figure 3. DGC mechanical representation and complete BG model.

$$y = (0 \ 0 \ 0 \ 0 \ 1) \begin{pmatrix} x_1 \\ x_2 \\ x_3 \\ x_4 \\ x_5 \end{pmatrix} \tag{6}$$

where Mse is the weigh force and  $x_5(t)$  represents the velocity of mass M2.

Since the DGC is made of latex, it is possible to control the pressure distribution on the foot sole by changing the shock absorbers density during manufacturing, that is, we can alter the dampers B2 and B3’s internal dynamic viscosity based on the patient’s physical characteristics and weight, which directly affect the relation between the shear stress and shear rate during gaiting (varying the Bi constants changes the position of the system’s poles in the spaces, and consequently its response).

### 2.4. Polynomial chaos

Polynomial chaos is a method to solve stochastic differential systems of the form [17]:

$$\dot{X}_t = F(X_t, W_t, \theta, c, t) \tag{7}$$

where  $\theta$  is a vector of random parameters in the probability space  $(\Omega, F, P)$ , generally independent and identically distributed;  $W_t$  is a stochastic process that represents an input to the system, also in  $(\Omega, F, P)$ ;  $c$  is a vector of initial conditions, that can also be a vector of random variables. The solution of Eq. (3) is a stochastic process  $(X_t, t \in T)$ , which is an uncountable collection of random variables in the same probability space  $(\Omega, F, P)$ , where T is the set of time instants. Another way to see the solution (or any other stochastic process) is through an application

$X: T \times \Omega \rightarrow \mathbb{R}^p$ , that is, a function of two variables  $X(t, \omega)$ , where  $\omega \in \Omega$  and is a particular result of the experiment. For each  $\omega$ , there is a time function called a trajectory. Normally, the regularity of  $X$  is only measurable in both variables. Supposing that  $X_t$  belongs to  $L_2(\Omega, F, P)$ , the Hilbert space of finite variance random variables, the method of polynomial chaos consists in expanding the solution of Eq. (3) into an orthogonal basis of this space. It was shown, in [18], that this expansion can be done for Gaussian processes by using Hermite polynomials, and, in [19], the method was extended to other standard probability distributions by using other polynomial basis (the Wiener-Askey scheme of polynomials). If there is only one independent random variable in Eq. (3), say  $\theta \in L_2(\Omega, F, P)$ , then all other functions of this random variable can be expanded as a Fourier series of the form.

$$f(\theta) = \sum_{i=0}^{+\infty} f_i \phi_i(\theta) \tag{8}$$

where  $\{\phi_i(\theta)\}$  is the orthogonal basis. It is known that in  $L_2(\Omega, F, P)$ , the internal product is given by:

$$E(fg) = \int p(\theta(\omega))f(\theta(\omega))g(\theta(\omega))dP(\omega) \tag{9}$$

where  $p(\theta)$  is the weight function (probability density function) and  $E(\phi_i(\theta)\phi_j(\theta)) = a_j \delta_{ij}$  and  $a_j$  are constants. The solution of Eq. (3) can then be expanded as

$$X(t, \omega) = \sum_{i=0}^{+\infty} X_i(t) \phi_i(\theta(\omega)) \tag{10}$$

where the coefficients  $X_i(t)$  are nonrandom time functions.

The system in Eq. (3) is then transformed into an infinite set of deterministic ordinary differential equations (one for each orthogonal polynomial). For numerical solutions, the series in Eq. (6) must be truncated, and the coefficients  $X_i(t)$  must be calculated by Galerkin projection [20]. So, the stochastic system in Eq. (3) can be approximated by a set of  $np$  ordinary differential equations, where  $n$  is the order of the stochastic system and  $p$  is the number of the polynomials in the Galerkin expansion. For systems with a set of random parameters  $\{\theta_i\}$ , with  $i = 1, \dots, n$  (independent of each other), multivariable polynomials can be used, which are also orthogonal and can be constructed by products of the single variable polynomials.

In this chapter, we analyze the case where only one system parameter is a variable, expressly the mass of the front region of the foot sole ( $M_1$ ). We assumed it is a random variable with uniform distribution and that the orthogonal polynomials for its weight function  $p(M_1)$  are the Legendre Polynomials  $L_i$  that satisfy

$$\int_{-1}^1 L_i(\theta) L_j(\theta) d\theta = \frac{2}{2j+1} \delta_{ij} \tag{11}$$

and can be calculated by the recursive formula found in [19], that is meaning standard probability distributions. Ten Legendre polynomials will be used, which means that the extended system of differential equations will have 50 equations. As the stochastic system in Eq. (3) is linear, the extended deterministic system will also be linear allowing us to analyze its eigenvalues/poles and zeros.

### 3. Results

#### 3.1. Bond graph modeling

The input data to solve the systems is represented by Eqs. (1) and (2) was obtained through the Emed n50 Novel platform’s static test. **Figure 4** shows the measurement apparatus as well as the mechanical model and pressure distribution on the fabricated latex-based insole. Two sensors were included in the forefoot—one to gather and the other to validate experimental data—since this is the area that experiences highest peak pressure values.

**Table 1** summarizes the data collected from each region of the subject’s right foot. The greatest variation of data occurred in the middle of the foot, indicating that the alteration in the COP and in the pressure distribution is caused by the neuropathy.

We used a Wiso W601 Digital 150 kg weighting scale to determine the center of mass, the weight, and the mass of the subject’s right foot. The measurements were taken using a double-support board, as suggested in [21]. The results were as follows: height = 1.72 m; weighting scale’s reading point in the board for the first measurement,  $T_a = 28.04 \pm 0.2$  m; weighting

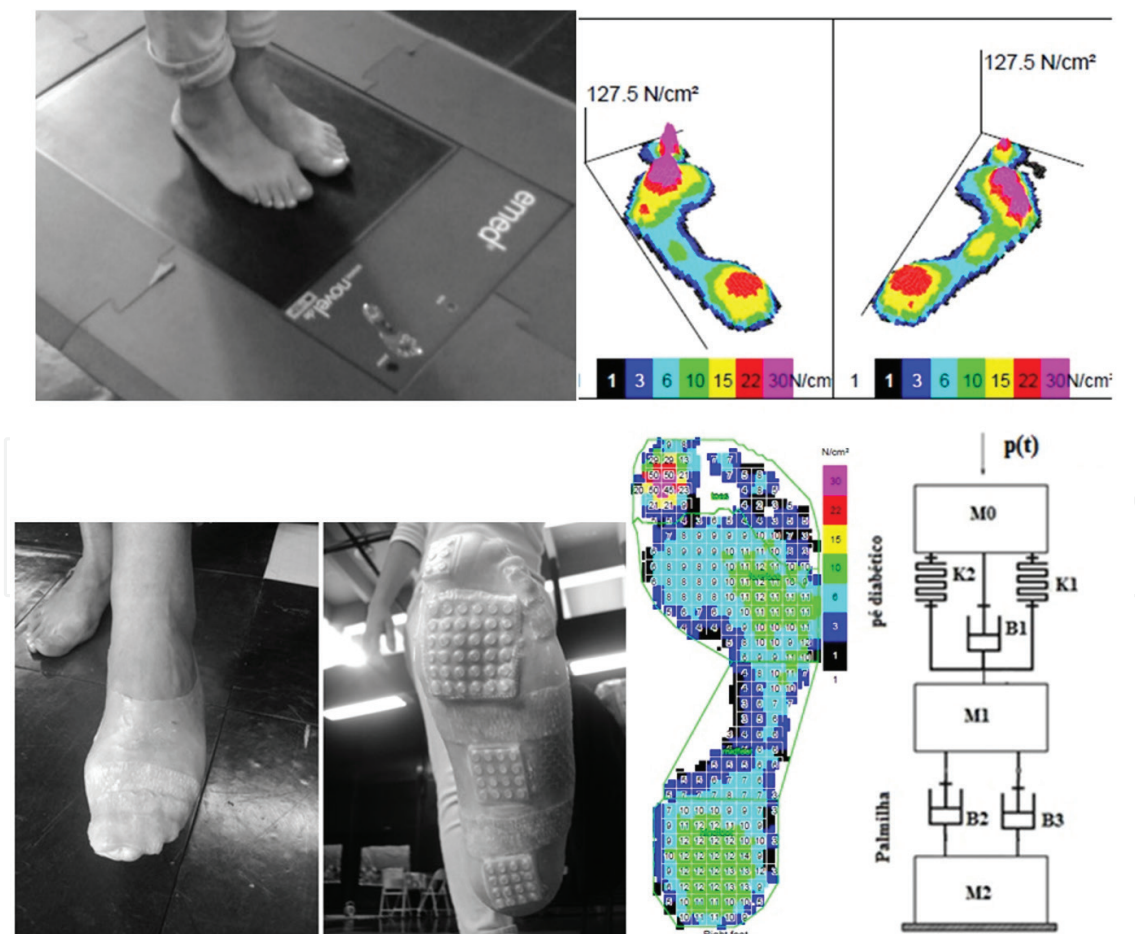


**Figure 4.** Insole prototype: Front side of insole’s shock absorbers—Right foot; cushioning system.

Parameters	Total	Hindfoot	Midfoot	Forefoot
Maximum force (N)	774.5 ± 28.8	465.0 ± 28.4	215.9 ± 18.6 <sup>1</sup>	682.1 ± 14.5
Peak pressure (N/cm <sup>2</sup> )	66.3 ± 18.2	30.9 ± 2.3	22.1 ± 5.8 <sup>2</sup>	65.8 ± 18.7
Contact time (%)	100.0 ± 0.0	58.0 ± 3.7	69.6 ± 2.6	84.3 ± 1.4
Contact area (cm <sup>2</sup> )	121.65 ± 2.74	33.65 ± 1.25	29.15 ± 0.40	49.05 ± 1.15
Comparative data: Right foot				
Maximum force (N)	768.5 ± 15.2	493.3 ± 12.5	121.7 ± 7.9	609.8 ± 13.9
Peak pressure (N/cm <sup>2</sup> )	54.0 ± 3.0	32.3 ± 1.0	11.6 ± 0.7	44.7 ± 2.5
Contact time (%)	100.0 ± 0.0	61.4 ± 1.0	61.0 ± 1.2	82.1 ± 0.7
Contact area (cm <sup>2</sup> )	135.03 ± 2.23	34.37 ± 0.59	27.13 ± 0.56	50.79 ± 0.84

<sup>1</sup>Higher measures than those from the comparative data.

<sup>2</sup>Higher measures than those from the comparative data.

**Table 1.** Experimental results of the static test obtained through the Emed n50 novel platform.

scale's reading point in the board for the second measurement,  $T'a = 27.0 \pm 0.2$  m; leg length,  $\ell = 0.65$  m; distance between the two supports,  $d = 1.61$ ; weight = 70 kg; center of mass (CM) position along the foot length direction member in relation to the nearest extremity,  $x_{CM} = 0.43$  cm; and calculated foot weight of  $M_0 = 7.6 \pm 1.2$  kg.

The parameters and constants used to solve the systems described by Eqs. (1) and (2) are listed in **Table 2**. Dynamic changes resulting from the introduction of the DGC were observed in the state space matrices of the system with DGC when compared with the one without DGC. It is noticed that the introduction of the DGC element alters the characteristic equation of the system, introducing phase lag and causing a damped system response when excited by a single step. This lag is a result of the reduction of the interaction of the foot with the surface.

Comparing the data captured by sensors S1 (identification) and S2 (validation), we tried to make a prediction of 10 future samples using the system model of Eq. (2). **Figure 5** shows, on its left, the prediction for 10 future samples, comparing between the estimated and the validation data. On the right, the image was zoomed and the original signal was introduced. We can observe that including the DCG element has provided a better behavioral pattern to represent the system of the diabetic gait.

Furthermore, **Figure 6a** and **b** shows the systems' responses for an impulse and a step input, respectively. We can clearly see a reduction in amplitude and oscillation in the DGC system's output signal when compared to the system without DGC.

### 3.2. Polynomial chaos analysis

All system parameters were assumed constant, except for the mass  $M_1$ , considered to be a uniformly distributed random variable with average value of 1.47 and standard deviation of 0.20 kg, conforming to **Table 1**. **Figure 7a** illustrates the resulting extended system

System's constants	Description of the variable	Obtainment	Value in SI and (CGS)
$V$	Displacement velocity of the shock absorber of the analogous system	It is considered to be the body velocity of the radial displacement (mm) of a diabetic barefoot person, obtained from the pressure platform and calculated with regard to the person's right foot.	0.01 [m] (1 cm)
$\alpha$	Constant that characterizes the decay of the static friction due to the viscosity of the latex	Adopted based on the inclination of the coagulation line of a slow particle.	$2.06 \cdot 10^{-7}$ [s/m] ( $2.06 \cdot 10^{-9}$ s/cm)
$B_1$	Coefficient of friction	The coefficient of friction corresponds to the ratio between the maximum friction force (weight force) and the intensity of the vertical force $N$ ( $\uparrow$ ) of the ground against the shoe's sole.	0.2 [N·s/m] (200 dyn·s/cm)
$B$	Negative and positive angles of inclination	Angle of inclination of the platform used to simulate the movement of going up or down steep regions.	$8^\circ$ ( $\pm 2^\circ$ ) (0.14 radians)
Cosine and sine	Indicates the relationship between the distance and the covered path.	Calculation of the cosine of the platform's angle of inclination.	-----
$M_0$	Mechanical stress concentrations in deep tissues of the plantar pad of the foot, may lead to foot ulceration, mass of foot	Ratio CM/length of the member in relation to the nearest extremity [21].	7.6 kg (7600 g)
$R$	The radius between the generated surface and the deflection ( $+\delta$ ), as shown in <b>Figure 2</b> .	Obtained with a normal gait surface, under the Axis of the Gait $-19^\circ$ in relation to the axis of the gait for a diabetic patient and a surface of $S = 0.0002 \text{ m}^2$ .	0.02 m (2 cm)
$G$	Gravitational acceleration	—	$9.8 \text{ m/s}^2$ (9800 $\text{cm/s}^2$ )
$K_1$	The elasticity of the human skin in the front region of the foot corresponds to the spring constant	Typical deformation curve, obtained by a Cutometer— $U_a/U_v$ [22], which, for this region, is of 0.633 mm, with the application of a weight force of 686 N.	$10.8 \cdot 10^{-5} \text{ N/m}$ (0.1080 dyn/cm)
$K_2$	Elasticity of the human skin in the region of the heel.	Typical deformation curve, obtained by a Cutometer— $U_a/U_v$ [22], which, for this region, is of 0.315 mm, with the application of a weight force of 686 N.	$22.1 \cdot 10^{-5} \text{ N/m}$ (0.2210 dyn/cm)
$M_1$	Mass of the front region of the plantar surface of the right foot bearing the body weight. The mass is obtained by the engraving of the foot's image on carbon paper.	Approximately oval area considered as an ellipsoid with $a = 4.8 \text{ cm}$ , $b = 3.5 \text{ cm}$ , and $c = 3.0 \text{ cm}$ (thickness of the foot). The volume obtained for the density of the skin was of $7 \text{ g/cm}^2$ .	$1.47 \pm 0.2 \text{ kg}$ (1470 g)
$M_{se} = fp$	Weight force	Measured by the force platform, Emed n50 Novel, with the patient standing in a double support static position.	686 N (680,000 dyn)
$B_2$	Coefficient of friction of the structural (or hysteretic) shock absorber, based on Eqs. (1) and (2). Damping is the process through which high pressure is removed from the system of the diabetic foot.	We measured it and multiplied it by the area of the shock absorber ( $\tau = \mu \cdot (v/t)$ ), being $v = 54.9 \text{ m/min}$ ( $\pm 12.0$ ), the diabetic patient's displacement velocity for a period of 2 min.	$6.4 \cdot 10^{-7}$ [N·s/m] ( $6.4 \cdot 10^{-4}$ dyn·s/cm)

System's constants	Description of the variable	Obtainment	Value in SI and (CGS)
$B_3$			$12.8 \cdot 10^{-7} [\text{N}\cdot\text{s}/\text{m}]$ ( $12.8 \cdot 10^{-4} \text{ dyn}\cdot\text{s}/\text{cm}$ )
$M_2$	Mass of the natural latex insole, including the shock absorbers.	Made of natural latex. Weighted with a digital weighting scale containing a high-precision sensor that identifies weight variations above 1 g.	0.007 kg (7 g)

**Table 2.** Parameters and constants for systems in Figures 2 and 3. The values in parenthesis were assumed to be uniformly distributed with 15% deviation from their nominal values. The simulation units are in the centimeter-gram-second (CGS) unit system.

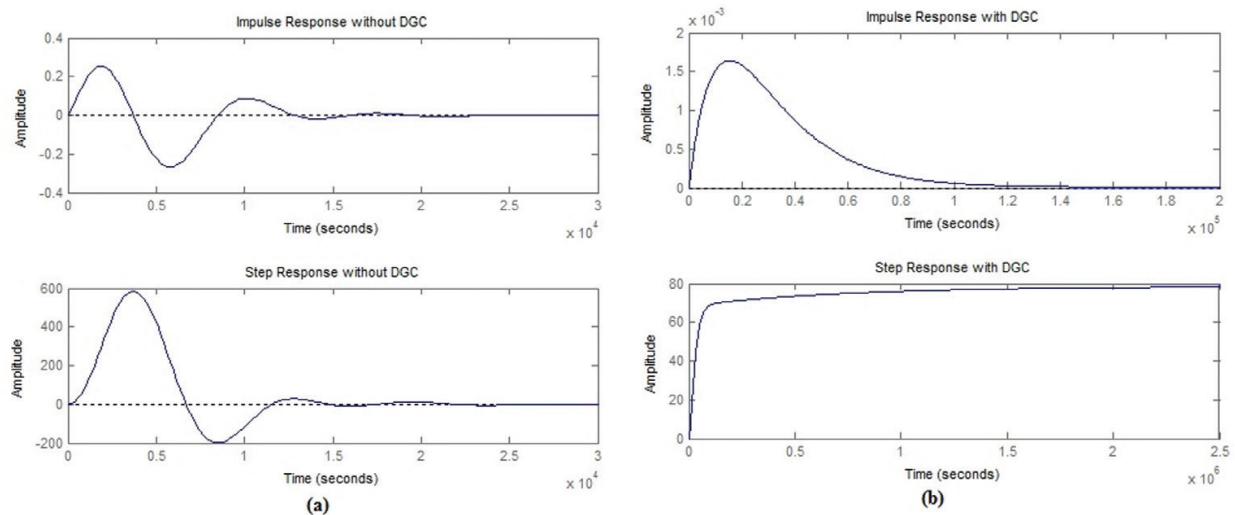


**Figure 5.** (a) Step response for both systems. (b) Impulse response for both systems.

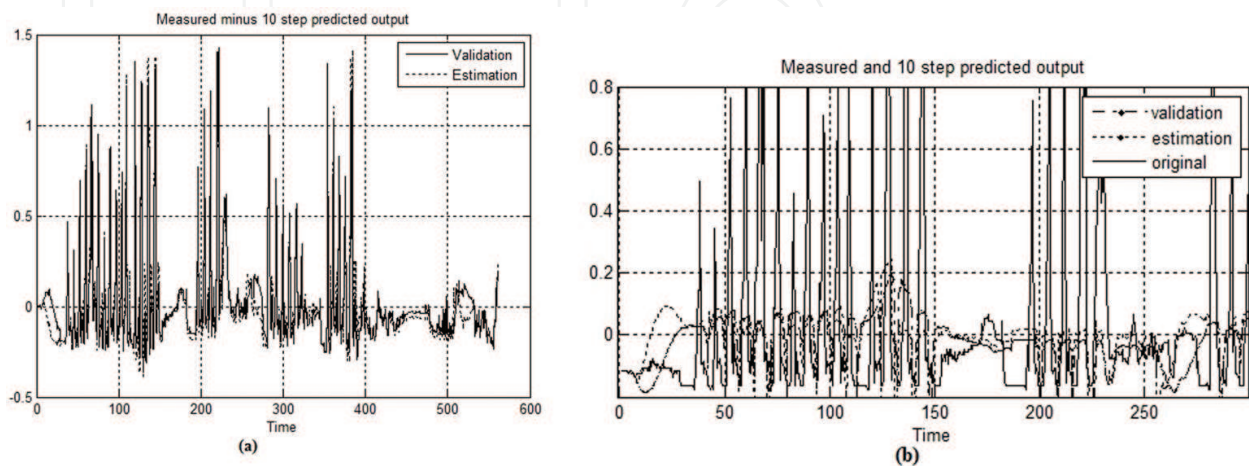


**Figure 6.** The plot shows an agreement between the different model structures and the data measured for validation. The unit of the Y-axis is in volts.

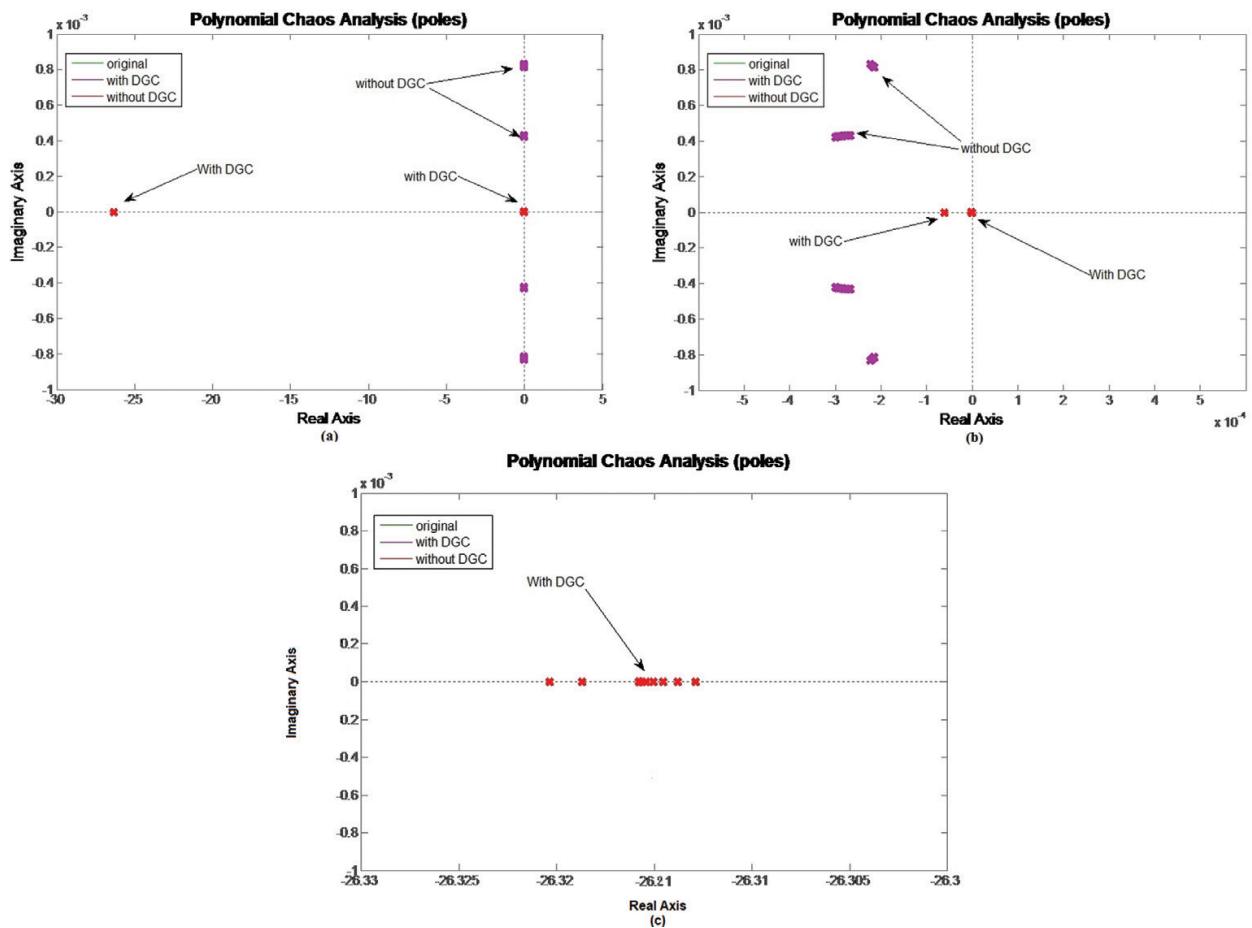


Figure 7. (a) Poles and zeros representation for the systems in Eqs. (1) and (2) using polynomial chaos analysis. (b) Zoomed portion of graph presented in Figure 7a. (c) Further zoom of the graph presented in Figure 7b.

poles (with and without DGC). This pole dispersion pattern represents the random of M1 for different feet (different people). From Figure 7b, we can conclude that the poles' variation was reduced in the presence of the DGC controller. Moreover, in Figure 7c and the zoomed version of Figure 7b, we can clearly see that the addition of DGC showed to be a good solution for the cancelation of the oscillatory behavior, besides making the system poles real. Finally, in Figure 6a, we can also see that an additional real pole appeared in -23.6, which was not present in the situation without DGC, which helps stabilize the system response. Therefore, the inclusion of the DGC in the system provides a more robust solution, with potential to benefit different kinds of feet (represented by differences in the mass M1).

#### 4. Discussion and conclusion

This chapter proposes the inclusion of an external element called *Diabetes Ground Control* (DGC), a personalized latex-based insole, aiming to correct the diabetic stride through the redistribution of the load on the foot. A mathematical model of the foot based on bond graph modeling was proposed with and without the inclusion of the DGC insole. The resulting DGC system was able to successfully predict the gaiting pattern for 10 future samples. In particular,

the proposed system reduced considerably the amplitude of foot pressure oscillations in foot sole during walking. In addition, a polynomial chaos analysis showed that the inclusion of the DGC element augmented the sensibility/robustness of the system. Hence, the DGC presents itself as a potential instrument to help controlling the tensions on the diabetic foot. Moreover, since the insole's shock absorbers can be fabricated with different dynamical viscosity values, the DGC element can be customized according to the patient's physical characteristics and weight, so everyone can receive the most efficient treatment based on his own gaiting pattern. The authors, after this result, will analyze the uncertainty of this mass of variables related to the patient, using quantifying uncertainty. Thus, the following result can provide a characterization of the eigenvalues of the problem solution in the presence of this uncertainty.

## Author details

Suélia de Siqueira Rodrigues Fleury Rosa<sup>1\*</sup>, Mário Fabrício Fleury Rosa<sup>2</sup>,  
Marcella Lemos Brettas Carneiro<sup>3</sup>, Leticia Coelho<sup>4</sup>, Diego Colón<sup>5</sup> and Célia Aparecida Reis<sup>6</sup>

\*Address all correspondence to: [suelia@unb.br](mailto:suelia@unb.br)

1 Faculdade do Gama, Universidade de Brasília (UnB), Brasília, Brazil

2 Doutorando em Ciências e Tecnologias em Saúde (PPGCTS), Faculdade de Ceilândia (FCE),  
Universidade de Brasília (UnB), Brasília, Brazil

3 Faculdade de Planaltina, Universidade de Brasília (UnB), Brasília, Brazil

4 Instituto de Física, Universidade de Brasília (UnB), Brasília, Brazil

5 Universidade de São Paulo (USP), São Paulo, Brazil

6 Departamento de Matemática, FC, UNESP, Bauru, Brazil

## References

- [1] Goske S, Erdemir A, Petre M, Budhabhatti S, Cavanagh PR. Reduction of plantar heel pressures: Insole design using finite element analysis. *Journal of Biomechanics*. 2006; **39**(13):2363-2370. DOI: <http://dx.doi.org/10.1016/j.jbiomech.2005.08.006>
- [2] Fábio Batista. *Uma Abordagem Multidisciplinar Sobre Pé Diabético*. 1st ed. São Paulo: Andreoli; 2010. 368 p. DOI: 9788560416110
- [3] Formosa C, Gatt A, Chockalingam N. The importance of clinical biomechanical assessment of foot deformity and joint mobility in people living with type-2 diabetes within a primary care setting. *Primary Care Diabetes*. 2013;**7**(1):45-50. DOI: 10.1016/j.pcd.2012.12.003
- [4] Kwon OY, Tuttle LJ, Johnson JE, Mueller MJ Muscle imbalance and reduced ankle joint motion in people with hammer toe deformity. *Clinical Biomechanics*. 2009;**24**(8):670-675. DOI: <http://dx.doi.org/10.1016/j.clinbiomech.2009.05.010>

- [5] El-Hilaly R, Elshazly O, Amer A. The role of a total contact insole in diminishing foot pressures following partial first ray amputation in diabetic patients. *The Foot*. 2013;**23**(1):6-10. DOI: 10.1016/j.foot.2012.10.002
- [6] Bowker J, Pfeifer M. Levin and O'Neal's the Diabetic Foot. 7th ed. Philadelphia: Mosby; 2008. 648 p. DOI: 9780323041454
- [7] Mueller MJ, Lott DJ, Hastings MK, Commean PK, Smith KE, Efficacy PTK. Mechanism of orthotic devices to unload metatarsal heads in people with diabetes and a history of plantar ulcers. *Physical Therapy*. 2006;**86**(6):833-842
- [8] Lawall H, Luedemann C, Amann B, Das TW. Diabetische Fußsyndrom [diabetic foot syndrome]. *Deutsche Medizinische Wochenschrift*. 2013;**138**(49):2503-2506
- [9] Rao S, Saltzman CL, Yack HJ. Relationships between segmental foot mobility and plantar loading in individuals with and without diabetes and neuropathy. *Gait and Posture*. 2009;**31**(2):251-255. DOI: 10.1016/j.gaitpost.2009.10.016
- [10] Martin RL, Irrgang JJ, Burdett RG, Conti SF, Van Swearingen JM. Evidence of validity for the foot and ankle ability measure (FAAM). *Foot & Ankle International*. 2005;**26**(11):968-983. DOI: 10.1177/107110070502601113
- [11] Raspovic A. Gait characteristics of people with diabetes-related peripheral neuropathy, with and without a history of ulceration. *Gait & Posture*. 2013;**38**(4):723-728. DOI: 10.1016/j.gaitpost.2013.03.009
- [12] Fernando M, Crowther R, Lazzarini P, Sangla K, Cunningham M, Buttner P, Golledge J. Biomechanical characteristics of peripheral diabetic neuropathy: A systematic review and meta-analysis of findings from the gait cycle, muscle activity and dynamic barefoot plantar pressure. *Clinical Biomechanics*. 2013;**28**(8):831-845. DOI: 10.1016/j.clinbiomech.2013.08.004
- [13] Piaggese A, Macchiarini S, Rizzo L, Palumbo F, Tedeschi A, Nobili LA, Leporati E, Scire V, Teobaldi I, Del Prato S. An off-the-shelf instant contact casting device for the management of diabetic foot ulcers: A randomized prospective trial versus traditional fiberglass cast. *Diabetes Care*. 2007;**30**(3):586-590. DOI: 10.2337/dc06-1750
- [14] Raspovic A, Landorf KB, Gazarek J, Stark M. Reduction of peak plantar pressure in people with diabetes-related peripheral neuropathy: An evaluation of the DH pressure relief shoe. *Journal of Foot and Ankle Research*. 2012;**5**:5-25. DOI: 10.1186/1757-1146-5-25
- [15] Suélia de Siqueira Rodrigues Fleury Rosa, Mirella Lorrainy Altoé. Bond graph modeling of the human esophagus and analysis considering the interference in the fullness of an individual by reducing mechanical esophageal flow. *Revista Brasileira de Engenharia Biomédica*. 2013;**29**(3). DOI: <http://dx.doi.org/10.4322/rbeb.2013.024>
- [16] Andrade TA, Iyer A, Das PK, Foss NT, Garcia SB, Coutinho-Netto J, Jordão-Jr AA, Frade MA. The inflammatory stimulus of a natural latex biomembrane improves healing in mice. *Brazilian Journal of Medical and Biological Research*. 2011;**44**(10):1036-1047. DOI: 10.1590/S0100-879X2011007500116

- [17] Fagiano L, Khammash M. Simulation of stochastic systems via polynomial chaos expansions and convex optimization. *Physical Review E*. 2012;**86**. DOI: 10.1103/PhysRevE.86.036702
- [18] Cameron RH, Martin WT. The orthogonal development of non-linear functionals in series of Fourier-Hermite functionals. *Annals of Mathematics*. 1947;**48**(2):385-392. DOI: 10.2307/1969178
- [19] Xiu D, Karniadakis GE. The Wiener-Askey polynomial chaos for stochastic differential equations. *SIAM Journal of Scientific Computing*. 2002;**24**(2):619-644. DOI: 10.1137/S1064827501387826
- [20] Fisher J, Bhattacharya R. Stability analysis of stochastic systems using polynomial chaos. In: *Proceedings of the 2008; 11-13 June 2008; Seattle, Wa, USA: IEEE; 2008*. DOI: 10.1109/ACC.2008.4587161
- [21] Veeger HEJ, Kai-Nan BJA, Rozendal RH. Parameters for modeling the upper extremity. *Journal of Biomechanics*. 1997;**30**(6):647-652. DOI: 10.1016/S0021-9290(97)00011-0
- [22] Dobrev HP. A study of human skin mechanical properties by means of Cutometer. *Folia Medica*. 2002;**44**(3):5-10

IntechOpen

